Evaluation of Downward Longwave Radiation in General Circulation Models

MARTIN WILD, ATSUMU OHMURA, AND HANS GILGEN

Swiss Federal Institute of Technology, Institute for Climate Research, Zurich, Switzerland

JEAN-JACQUES MORCRETTE

European Centre for Medium-Range Weather Forecasts, Reading, Berkshire, United Kingdom

ANTHONY SLINGO

Hadley Centre for Climate Prediction and Research, Met Office, Bracknell, Berkshire, United Kingdom

(Manuscript received 26 April 2000, in final form 10 October 2000)

ABSTRACT

The longwave radiation emitted by the atmosphere toward the surface [downward longwave radiation (DLR)] is a crucial factor in the exchange of energy between the earth surface and the atmosphere and in the context of radiation-induced climate change. Accurate modeling of this quantity is therefore a fundamental prerequisite for a reliable simulation and projection of the surface climate in coupled general circulation models (GCM).

DLR climatologies calculated in a number of GCMs and in a model in assimilation mode (reanalysis) are analyzed using newly available data from 45 worldwide distributed observation sites of the Global Energy Balance Archive (GEBA) and the Baseline Surface Radiation Network (BSRN). It is shown that substantial biases are present in the GCM-calculated DLR climatologies, with the GCMs typically underestimating the DLR (estimated here to be approximately 344 W m^{-2} globally). The biases are, however, not geographically homogeneous, but depend systematically on the prevailing atmospheric conditions. The DLR is significantly underestimated particularly at observation sites with cold and dry climates and thus little DLR emission. This underestimation gradually diminishes toward sites with more moderate climates; at sites with warm or humid atmospheric conditions and strong DLR emission, the GCM-calculated DLR is in better agreement with the observations or even overestimates them. This is equivalent to creating an excessively strong meridional gradient of DLR in the GCMs.

The very same tendencies are independently found in stand-alone calculations with the GCM radiation codes in isolation, using observed atmospheric profiles of temperature and humidity for cloud-free conditions as input to the radiation schemes. A significant underestimation of DLR is calculated by the radiation schemes when driven with clear-sky atmospheric profiles of temperature and humidity representative for cold and dry climates, whereas the DLR is no longer underestimated by the radiation schemes with prescribed clear-sky profiles representative for a hot and humid atmosphere. This suggests that the biases in the GCM-calculated DLR climatologies are predominantly induced by problems in the simulated emission of the cloud-free atmosphere.

The same biases are also found in the DLR fluxes calculated by the European Centre for Medium-Range Weather Forecasts (ECMWF) model in assimilation mode (reanalysis), in which the biases in the atmospheric thermal and humidity structure are minimized. This gives further support that the biases in the DLR are not primarily due to errors in the model-predicted atmospheric temperature and humidity profiles that enter the radiative transfer calculations, but rather are due to the radiation schemes themselves. A particular problem in these schemes is the accurate simulation of the thermal emission from the cold, dry, cloud-free atmosphere.

1. Introduction

The exchange of energy between the atmosphere and ocean or land surfaces in the longwave is based on the thermal emission of the earth's surface and the atmospheric emission directed to the surface (incoming longwave radiation or downward longwave radiation, hereinafter referred to as DLR). These fluxes are the two largest components of the globally averaged surface energy balance, which is therefore very sensitive to deficiencies in their parameterizations. While the modeling of the thermal emission of the surface is straightforward according to the Stefan–Boltzmann law, the DLR has to be determined by comprehensive radiative transfer calculations that take into account the complex radiative characteristics of the atmosphere.

Ma et al. (1994) showed that coupled atmosphere–ocean general circulation models (GCMs) are highly

Corresponding author address: Martin Wild, Swiss Federal Institute of Technology, Institute for Climate Research, Winterthurerstr. 190, CH-8057 Zurich, Switzerland.
E-mail: wild@geo.umnw.ethz.ch

© 2001 American Meteorological Society

Unauthenticated | Downloaded 05/28/23 05:15 PM UTC

sensitive to the choice of the parameterization of the DLR. Despite its importance in climate system modeling, the simulation of DLR in the current generation of GCMs is still afflicted with large uncertainties, resulting in substantial differences in the calculated fluxes among the various GCMs (Gutowski et al. 1991; Randall et al. 1992; Wild et al. 1995a, 1998; Garratt and Prata 1996). Over the years, this large disparity remained relatively unquestioned because of the absence of an adequate observational reference. Unlike the longwave radiation emitted to space, which is by now well established through satellite measurements (Harrison et al. 1990), the longwave exchanges at the earth–atmosphere interface have not been well determined from observations. Because of the difficulties involved in the measurements of DLR, this quantity has for long only been observed at few sites. A first attempt to verify DLR in GCMs was made by Wild et al. (1995a,b) using direct observations gathered in the Global Energy Balance Archive (GEBA; Ohmura et al. 1989; Gilgen and Ohmura 1999). Based on the limited data available, Wild et al. (1995a) presented evidence that the DLR is typically too small in GCMs. Similar results were obtained in the study by Garratt and Prata (1996), using largely the same data but other GCMs.

In the meantime, the observational information on DLR has significantly improved, mainly because of the efforts within the Baseline Surface Radiation Network (BSRN/WCRP; Ohmura et al. 1998), whose data center is located at the first author's institute. The BSRN aims at providing observations of surface radiation fluxes of the best possible quality and high sampling rate. In light of the recent availability of new observational data from BSRN and from updates in the GEBA database, a reevaluation of the GCM-calculated fluxes of downward radiation has become necessary. In particular, the available data now allow an assessment of the GCM fluxes in highly contrasting climate regions, as will be demonstrated in the present study.

2. Models

The longwave fluxes from four GCMs and from one model in assimilation mode are investigated in detail in the present study: the ECHAM3 and ECHAM4 models from the Max Planck Institute for Meteorology, Hamburg, Germany (Roeckner et al. 1992, 1996), and the HadAM2b and HadAM3 models from the Hadley Centre for Climate Prediction and Research, Bracknell, United Kingdom (Stratton 1999; Pope et al. 2000). The model data stem from Atmospheric Model Intercomparison Project–type simulations with prescribed SST and sea ice for the period 1979–88. The experiments were done at the highest horizontal resolution currently feasible: T106 or 1.1° for ECHAM3 and ECHAM4 and $0.833° \times 1.25°$ for the HadAM2b gridpoint model, except that HadAM3 was only available at standard resolution ($2.5° \times 3.75°$) for this study. The effect of increased resolution on the results in HadAM3 is currently being investigated. The high horizontal resolution facilitates the comparison with point observations and minimizes the differences in altitude between the GCM grid points and the observation site, on which the DLR is rather sensitive (Wild 1997). From the European Centre for Medium-Range Weather Forecasts (ECMWF), Reading, United Kingdom, the longwave fluxes of the ECMWF reanalysis (ERA) dataset is additionally included, obtained by the ECMWF model in assimilation mode (Gibson et al. 1997). These fluxes were available for the period 1985–93 and have the same horizontal resolution as the GCMs (T106). The fluxes from reanalyses have further the distinct advantage that the best possible estimates of the meteorological quantities in the overlying atmosphere were taken into account for their calculations.

All models include broadband radiation schemes with two-stream approximation as typically used in GCMs. The transition from the second-latest to the latest model versions in both the HadAM and ECHAM model series included the replacement of the radiation schemes. Thus, the four GCMs used in this study include four independent radiation schemes, which may reflect the status of radiation modeling typical for the current generation of GCMs. The radiation schemes are described in detail in Slingo and Wilderspin (1986) for HadAM2b, Edwards and Slingo (1996) for HadAM3, Hense et al. (1982) for ECHAM3, Morcrette et al. (1986) for ERA, and Morcrette et al. (1986) with modifications according to Giorgetta and Wild (1995) for ECHAM4.

3. Observational data

The observational data for the assessment of the GCM-calculated DLR have been retrieved from two databases established at the Swiss Federal Institute of Technology: GEBA (Ohmura et al. 1989; Gilgen and Ohmura 1999) and BSRN (Ohmura et al. 1998). GEBA is a database for the worldwide measured energy fluxes at the earth's surface and contains monthly mean values of the various surface energy balance components. While the best-documented component in GEBA is the shortwave downward radiation (Gilgen et al. 1998), this database also contains a limited number of sites with DLR measurements suitable for the purposes of the present study. The database of the BSRN includes DLR measurements at high temporal resolution (minute values) with the highest possible accuracy at selected sites in different climate regions. Additionally, synoptic measurements and upper-air soundings from radiosondes are stored at these sites, which constitute an ideal test bed for the validation of radiation codes. In total, 45 observation sites have been brought together for the present study. They are compiled in Table 1, including their positions, altitudes, observation periods, and data sources. Twenty-six sites are taken from GEBA, including the ones with the longest measurement records, that is, Hamburg, Germany (36 yr),

Unauthenticated | Downloaded 05/28/23 05:15 PM UTC

TABLE 1. Observation sites used in this study, ordered by decreasing latitude.

Station	Lat	Long	Altitude	Obs period	Source
Axel Heiberg Island	79.68°N	90.45°W	1530	1960	GEBA
Ny Alesund, Spitsbergen	78.56°N	11.56°E	10	1992–99	BSRN
Cape Abernathy	77.75°N	101.17°W	20	1973	GEBA
Barrow, Alaska	71.27°N	156.83°W	10	1992–97	BSRN
Camp4 EGIG, Greenland	69.67°N	49.63°W	1004	1959	GEBA
Bergen, Norway	60.40°N	5.32°E	45	1965–89	GEBA
Schleswig, Germany	54.53°N	9.55°E	59	1984–89	GEBA
Hamburg, Germany	53.65°N	10.12°E	49	1954–89	GEBA
Braunschweig, Germany	52.30°N	10.45°E	81	1989	GEBA
Cabauw, The Netherlands	51.96°N	4.93°E	0	1987	*
Regina, Canada	50.12°N	104.43°W	578	1996	BSRN
NE Pacific	50.00°N	140.00°W	0	1980	GEBA
Geisenheim, Germany	49.98°N	7.95°E	131	1988–89	GEBA
Stuttgart, Germany	48.83°N	9.20°E	318	1988–89	GEBA
Weihenstephan, Germany	48.40°N	11.72°E	469	1987–89	GEBA
Hartheim, Germany	47.93°N	7.62°E	201	1974–85	GEBA
Basel-Binningen, Switzerland	47.58°N	7.58°E	317	1978–81	GEBA
Reckenholz, Switzerland	47.43°N	8.52°E	443	1988–94	GEBA
Rietholzbach, Switzerland	47.38°N	9.00°E	760	1988–94	GEBA
Weissfluhjoch, Switzerland	46.82°N	9.83°E	2677	1958–59	GEBA
Payerne, Switzerland	46.82°N	6.95°E	491	1992–99	BSRN
Arosa, Switzerland	46.78°N	9.68°E	1818	1990–94	GEBA
Davos, Switzerland	46.80°N	9.82°E	1580	1958–59	GEBA
Carpentras, France	44.05°N	5.03°E	100	1996–99	BSRN
Boulder, Colorado, United States	40.03°N	105.27°W	1577	1992–97	BSRN
Billings, Montana, United States	36.36°N	97.50°W	317	1995–97	BSRN
Tateno, Japan	36.03°N	140.08°E	25	1996–99	BSRN
Western North Pacific	35.00°N	139.00°E	0	1981–85	GEBA
Bermuda	32.30°N	64.75°W	10	1992–97	BSRN
Nansei Islands, Pacific Ocean	23.50°N	128.00°E	0	1974–75	GEBA
Kwajalein, Marshall Islands	8.72°N	167.73°E	10	1993–98	BSRN
Illorin, Nigeria	8.32°N	4.34°E	350	1992–94	BSRN
Manaus, Brazil	2.95°S	59.95°W	26	1983–85	†
Kinshasa, Zaire	4.35°S	15.25°E	450	1959	GEBA
Alice Springs, Australia	23.70°S	133.87°E	547	1995–98	BSRN
Florianopolis, Brazil	27.53°S	48.52°W	11	1994–99	BSRN
Uardry, Australia	34.39°S	145.30°E	94	1992–97	#
Syowa, Antarctica	69.00°S	39.59°E	3	1994–96	BSRN
Nishinoura, Antarctica	69.00°S	39.55°E	0	1980	GEBA
Pionerskaya, Antarctica	69.73°S	95.50°E	2740	1956–58	GEBA
Georg von Neumayer, Antarctica	70.39°S	8.15°W	42	1992–99	BSRN
Mizuho, Antarctica	70.39°S	44.33°E	2230	1977–80	GEBA
Little America 5, Antarctica	78.18°S	162.17°W	44	1957–58	GEBA
Plateau Station, Antarctica	79.25°S	40.50°E	3630	1967	GEBA
Amundsen–Scott, Antarctica	90.00°S	—	2841	1992–97	BSRN

* Van Ulden and Wieringa (1996)
† Shuttleworth (1988)
# Prata et al. (1998)

and Bergen, Norway (25 yr). Nineteen BSRN stations are now operational and report their data to the first author's institute. Sixteen of these sites have by now observational records of sufficient length to be included in the present study. The latest status of BSRN is used here, with measurement records running well into the 1999. Three additional sites are taken from other sources as referenced in Table 1. The global distribution of the sites used in this study is illustrated in Fig. 1. As compared with the earlier studies, the geographical coverage with observation sites has not only been improved in mid- and high latitudes, but due to the new BSRN data particularly, also in low latitudes, where no observations were previously available.

The observational records of the various sites do not necessarily cover identical periods (cf. Table 1). Thus the assumption of stationarity is adopted for the comparisons with the models throughout the study. This assumption is not unfounded for the past decades covered by the measurements. The greenhouse forcing over this period is estimated to be less than 2 W m^{-2} per decade (Wild et al. 1997) and is thus smaller than the measurement uncertainties. Furthermore the DLR at a site is not overly sensitive to the variability in synoptic weather conditions due to two counterbalancing effects: years with an excessive frequency of synoptic disturbances tend to be cooler and more cloudy, which induces less-than-average emission from the cooler cloud-free atmosphere but

Unauthenticated | Downloaded 05/28/23 05:15 PM UTC

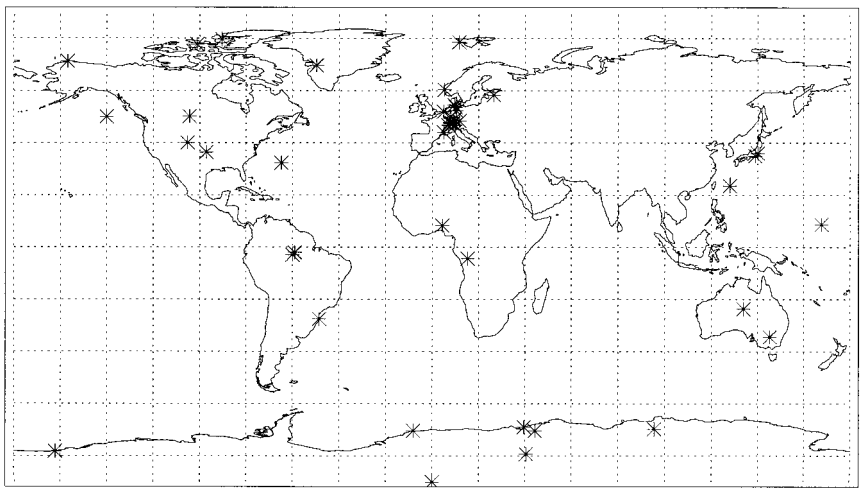

FIG. 1. Global distribution of the 45 observation sites with DLR measurements used in this study.

more-than-average emission from clouds, and vice versa for years with little synoptic disturbances. This results in a small interannual variability and in time series with small standard deviation as can be seen in Table 2. No major long-term trends can also be noted in the long time series of DLR in GEBA, as can be deduced from the small standard deviations given in Table 2.

An investigation is in progress to estimate the measurement uncertainty from a long-term instrument comparison experiment jointly performed by the first author's institute and the Swiss Meteorological Institute. The current best estimate for the DLR measurement error is ± 10 W m^{-2}, based on the studies of Deluisi et al. (1992), Philipona et al. (1998), and references therein. The accuracy of DLR measurements according to BSRN standards is now about 2–3 W m^{-2} (Ohmura et al. 1998).

4. Results

The uncertainties in the simulation of DLR in current GCMs are readily apparent in a simple comparison of their global means. This is shown in Fig. 2, where the mean DLR calculated with different GCMs is displayed. Their values vary largely, covering a range of more than 40 W m^{-2}. This is more than 2 times the magnitude of the expected change in DLR at the time of doubled CO_2 (Wild et al. 1997). To obtain more insight into these discrepancies, the GCM-calculated flux climatologies are evaluated against the observational references in a pointwise comparison.

For the comparison of GCM fluxes with those observed at the 45 sites given in Table 1, the model data were interpolated to the measurement sites using the four surrounding grid points weighted by their inverse spherical distance. Ocean grid points that may surround the sites have not been taken into account. The high

TABLE 2. Long-term annual mean and standard deviation of DLR (W M^{-2}) for selected sites.

Station	Means ± std dev	Period
Hamburg, Germany	326 ± 3.2	1955–93
Bergen, Norway	317 ± 5.1	1965–95
Tateno, Japan	330 ± 5.0	1977–95
Payerne, Switzerland	318 ± 2.7	1988–96
Reckenholz, Switzerland	325 ± 2.2	1989–97
Rietholzbach, Switzerland	320 ± 5.0	1989–97

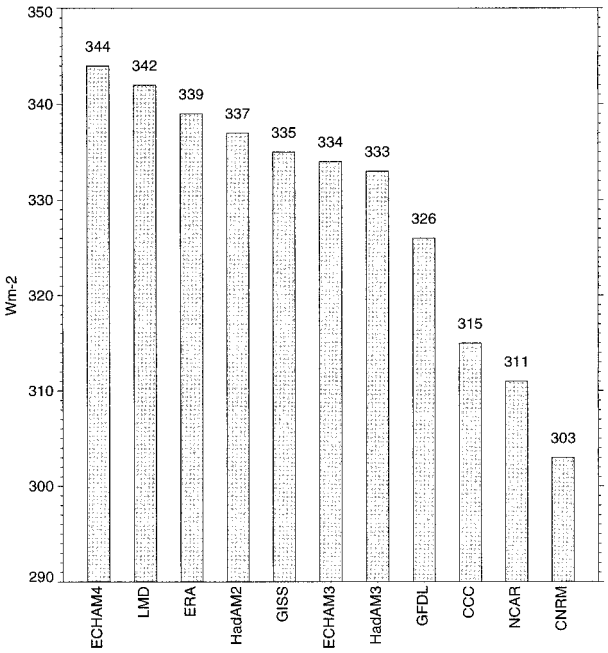

FIG. 2. Global annual mean DLR (W m^{-2}) in various GCMs and ERA.

Unauthenticated | Downloaded 05/28/23 05:15 PM UTC

TABLE 3. Long-term annual mean values of DLR (W m^{-2}) averaged over the 45 sites as observed and as calculated in the GCMs.

Observed	294
ECHAM3	284
ECHAM4	292
HadAM2b	284
HadAM3	283
ERA	280

horizontal resolution of the models (~1.1°) facilitates a comparison with point measurements as compared with coarser-resolution GCMs, because of more realistic coastlines and topography. This prevents, for example, observation sites on land from being located in ocean areas in the model and reduces the altitudinal differences between the model grid points and the observational sites in nonflat terrain. Still, also for the high-resolution models, a correction has to be applied whenever the elevation of the observation sites and the corresponding model grid points differ significantly, since DLR shows a strong dependence on altitude (Wild et al. 1995b; Wild 1997). The altitudinal correction applied here is based on the study of Wild et al. (1995b); where substantial height differences between model and real topography exist, a height correction of 2.8 W m^{-2} per 100 m was applied. This height gradient was derived from the Swiss radiation network with three stations for DLR at different heights in the Alps. Because of the high resolution of the GCMs, the height correction was marginal at most sites.

Long-term annual mean values of DLR observed at the 45 sites are compared with the respective model fluxes in Table 3. This table contains simple averages over the model-calculated and observed fluxes at the 45 sites. Note that these averages are smaller than the corresponding global means in Fig. 2 because of the dominance of the higher-latitude sites in the dataset considered here. The GCMs calculate generally lower values than the observations suggest, in the range of 2 W m^{-2} (ECHAM4) to 14 W m^{-2} (ERA). The negative biases found in the GCM DLR fluxes are in line with the previous studies of Wild et al. (1995a,b) and Garratt and Prata (1996). However, the considerably enlarged observational database in comparison with these earlier studies allows now a more differentiated investigation of the bias structure. This is shown in Fig. 3, where the long-term means at each individual observation site are compared against the corresponding GCM fluxes for the four GCMs. A distinct common structure in the model biases becomes apparent. The fluxes with small absolute values, stemming from sites in cold and dry climates, are significantly underestimated, while the fluxes with higher absolute values from warm humid climates are closer to the observations or are even overestimated in some of the models. This is also seen in the linear least squares fits between observed and model-calculated DLR given in Fig. 3. The slopes of the linear regression lines are consistently larger than 1 in all models (with a slope equal to 1 representing a perfect match). Thus, the magnitude and even the sign of the biases depend on the prevailing atmospheric conditions. Problems in the simulated DLR become particularly evident under cold and dry climates, in line with the studies of Wild et al. (1995a,b) and Garratt and Prata (1996), which were based on mid- and high-latitude stations only. At low-latitude sites, which were not considered in these studies, the biases are, however, reduced (ECHAM3, HadAM3) or even slightly reversed (ECHAM4, HadAM2b).

This is further illustrated in Figs. 4 and 5, where annual cycles of DLR of some of the most reliable sites for the different latitude zones are shown together with the corresponding model fluxes (ECHAM models in Fig. 4, HadAM models in Fig. 5). The DLR at the high- and midlatitude sites are mostly underestimated throughout the year by all models, while the DLR at the lower-latitude sites are in better agreement (ECHAM3, Fig. 4; HadAM3, Fig. 5) or even overestimated (ECHAM4, Fig. 4; HadAM2b, Fig. 5). The above findings also imply that a common problem in the GCMs is a meridional gradient of DLR that is too strong. This is found in all models investigated here independent of the absolute magnitude of their fluxes. The excessive meridional gradient of DLR may have a deteriorating effect on the simulated meridional temperature distribution and associated atmosphere and ocean dynamics.

5. Discussion

The origins of the DLR biases may be due to (i) inaccuracies in the formulation of the radiation scheme, or (ii) inaccuracies in the GCM-predicted atmospheric properties that enter the radiation scheme. These two aspects are further investigated in the following sections.

a. Assessment of radiation schemes in stand-alone mode

To estimate the contribution from the radiation scheme itself to the biases detected above, the performance of the radiation schemes in the ECHAM models is assessed separately from the rest of the GCM in stand-alone mode. In this approach, the stand-alone radiation calculations are done using observed atmospheric water vapor and temperature profiles from radiosondes instead of the ones predicted by the GCM as input. Thereby, possible biases in the GCM-predicted atmospheric temperature and humidity structure as sources for the flux deficiencies can be eliminated (Wild et al. 1995a). This method then allows for an appropriate validation of the calculated DLR with synchronous collocated surface measurements under identical atmospheric conditions. For such a validation exercise, observation sites with both radiation measurements and collocated upper-air sounding facilities are necessary. The BSRN stations

Unauthenticated | Downloaded 05/28/23 05:15 PM UTC

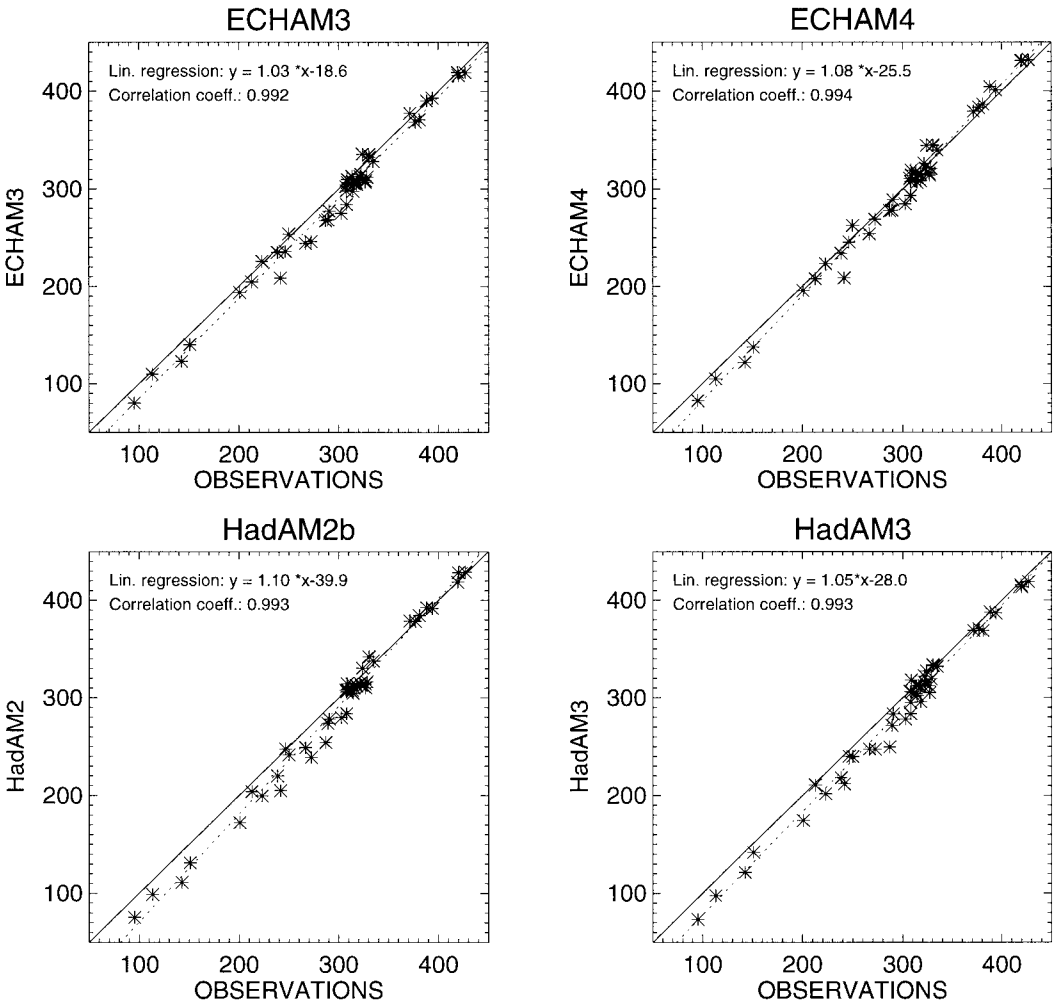

FIG. 3. Annual mean DLR (W m^{-2}) calculated with the HadAM2, HadAM3, ECHAM3, and ECHAM4 models vs observations at the 45 sites displayed in Fig. 1 and Table 1.

are designed to fulfill these requirements. For the present study, data from three BSRN stations in contrasting climate regimes are included: Neumayer (Antarctica), Payerne, Switzerland (midlatitudes), and Kwajalein, (tropical Pacific, cf. Table 1). Additionally, a similar dataset from the ETH Camp Greenland (Ohmura et al. 1994) that fulfills the BSRN standards is used. Results from stand-alone calculations with the radiation schemes used in two of the GCMs (ECHAM3, ECHAM4) at these four sites are merged into Fig. 6. Only clear-sky conditions are considered to avoid the uncertainties introduced with the specification of cloud parameters. The smallest fluxes in Fig. 6 stem from the Antarctic site, while the highest values are from the tropical site, Kwajalein. A striking feature can be noted. The instantaneous clear-sky calculations with the isolated radiation schemes show very similar biases as found before in the long-term (all sky) climatologies calculated with the full GCMs at the 45 sites. The fluxes with low absolute values stemming from the cases with data from the high-latitude sites are underestimated in the stand-alone calculations, while they are in better agreement or overestimated for the tropical cases. The biases in Figs. 3 and 6 are consistent despite the fact that they are based on independent datasets and approaches. While Fig. 3 is based on a comparison of long-term mean all-sky climatologies at a large number of sites, Fig. 6 includes instantaneous clear-sky comparisons from four selected sites. Both type of comparisons result also in very similar slopes in their linear least square fits, as given in Figs. 3 and 6. The striking similarity of Figs. 3 and 6 is a strong hint that the biases found above in the GCM-calculated all-sky climatologies at the 45 sites are largely determined by biases in the emission of the cloud-free atmosphere calculated by the radiation scheme in these models. The biases in the clear-sky fluxes remain fully apparent also under all-sky conditions, since most of the DLR originates from the lowest atmospheric layers below cloud level, making the cloud forcing essentially an add-on to the clear-sky DLR.

Unauthenticated | Downloaded 05/28/23 05:15 PM UTC

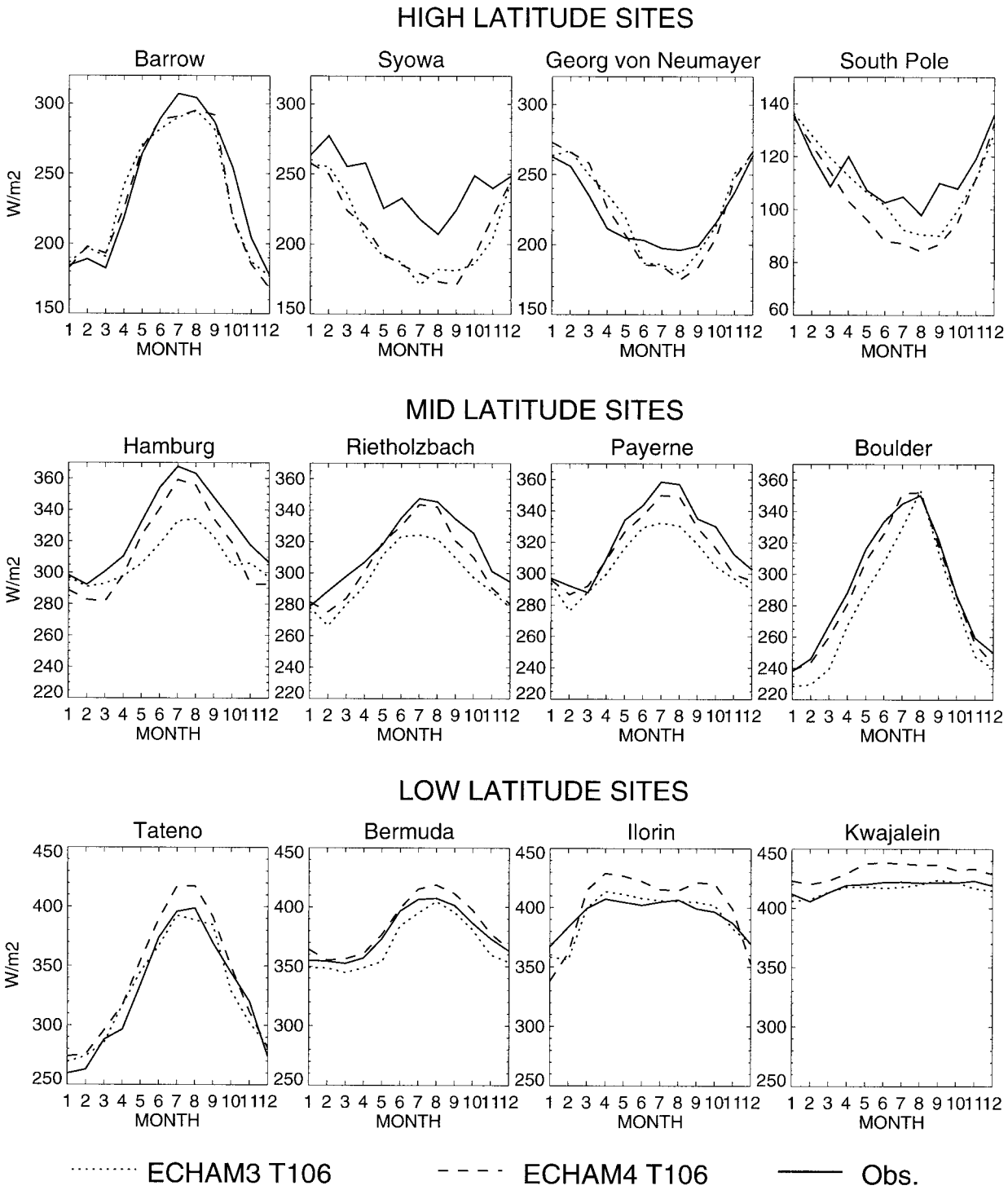

FIG. 4. Annual cycles of model-calculated and observed DLR (W m^{-2}) at some of the most reliable high-latitude sites, midlatitude sites, and low-latitude sites (see Table 1 for more information on these sites): model calculations by ECHAM3 (dotted) and ECHAM4 (dashed), and observed (solid).

Unauthenticated | Downloaded 05/28/23 05:15 PM UTC

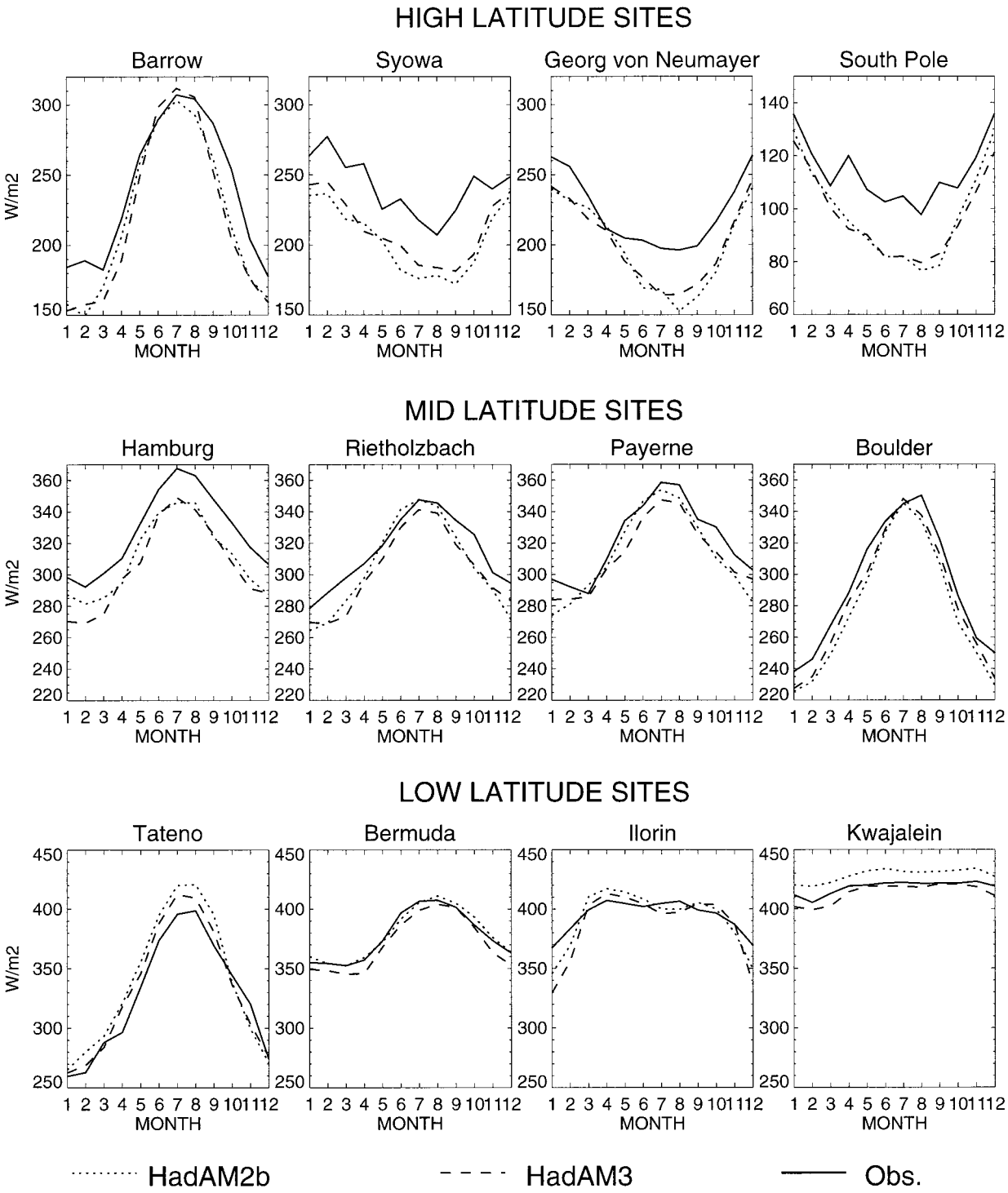

FIG. 5. As Fig. 4, but model calculations by HadAM2b (dotted) and HadAM3 (dashed).

Thus, the biases in the performance of the radiation schemes under cloud-free conditions seem to be also a primary factor for the overly strong meridional gradient of DLR in the models. A particular problem appears to be the simulation of insufficient emission from the cold dry atmosphere.

b. Comparisons with reanalysis

In addition to the problems intrinsic to the GCM radiation schemes as outlined above, biases in the DLR may be introduced through biases in the GCM-predicted thermal and humidity structure in the atmosphere, which

Unauthenticated | Downloaded 05/28/23 05:15 PM UTC

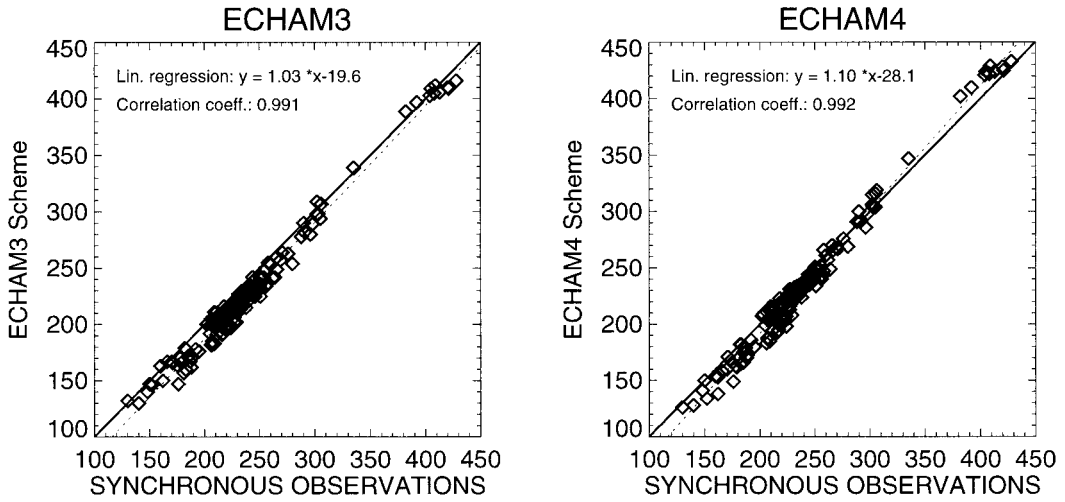

FIG. 6. Offline calculations with the isolated radiation codes of the ECHAM3 and ECHAM4 models. Shown are calculated DLR (W m^{-2}) using prescribed profiles of atmospheric temperature and humidity from radiosonde data vs synchronous surface observations for clear-sky conditions.

enters the radiative transfer calculations. It is therefore instructive to analyze also the DLR calculated in the ERA (Gibson et al. 1997), where biases in the atmospheric structure are minimized. The ERA dataset was constructed through a repetition of the numerical weather forecast cycles over the period 1979–93, where the worldwide data from the Global Observing System were assimilated and physically interpolated with the ECMWF model in 6-hourly intervals. This results in what is believed to be the best current estimate of the humidity and temperature structure in the atmosphere. Therefore, the DLR fluxes calculated in the ERA have the advantage that they are less likely deteriorated by biases in the atmospheric temperature and humidity structure than in GCMs. The same applies for the two other reanalysis datasets produced at the National Centers for Environmental Prediction and at the National Aeronautics and Space Administration's Goddard Laboratory for Atmospheres. The long-term annual mean DLR fluxes calculated in ERA are compared with the 45 observation sites in Fig. 7a. Despite the accurate consideration of the atmospheric temperature and humidity structure, the biases are not reduced and are still very similar to the GCMs in Fig. 3. The underestimation is again particularly evident at sites with low absolute flux values. Similar biases as before with the GCMs also become apparent in the comparison of the seasonal climatologies at the selected sites in Fig. 8: while the dry high-latitude sites show a significant underestimation, the moist tropical sites with larger fluxes are in

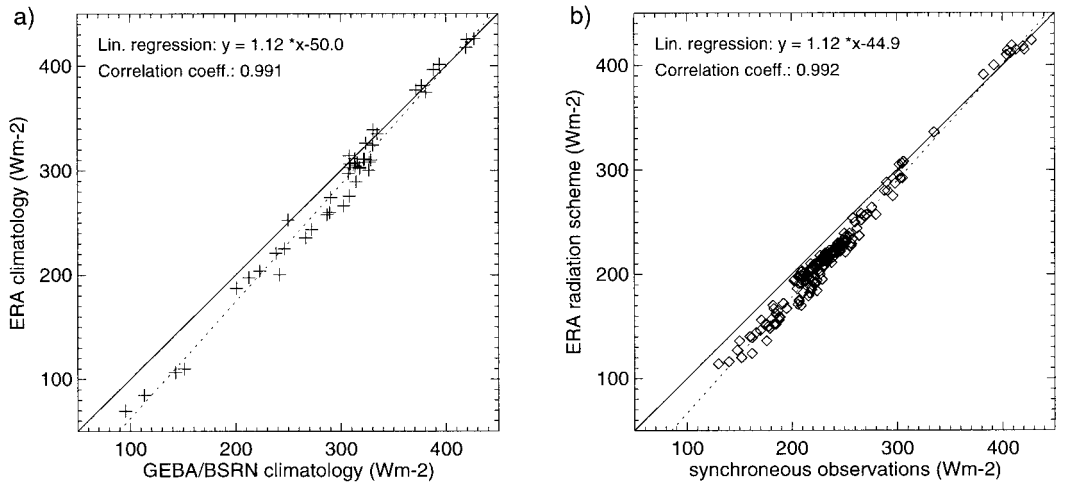

FIG. 7. (a) Long-term annual mean DLR (W m^{-2}) calculated in the ECMWF reanalysis vs observations at 45 sites from GEBA and BSRN. (b) Instantaneous offline calculations with the isolated radiation codes of the ECMWF reanalysis for clear-sky conditions: calculated DLR using prescribed profiles of atmospheric temperature and humidity from radiosonde data vs synchronous surface observations.

Unauthenticated | Downloaded 05/28/23 05:15 PM UTC

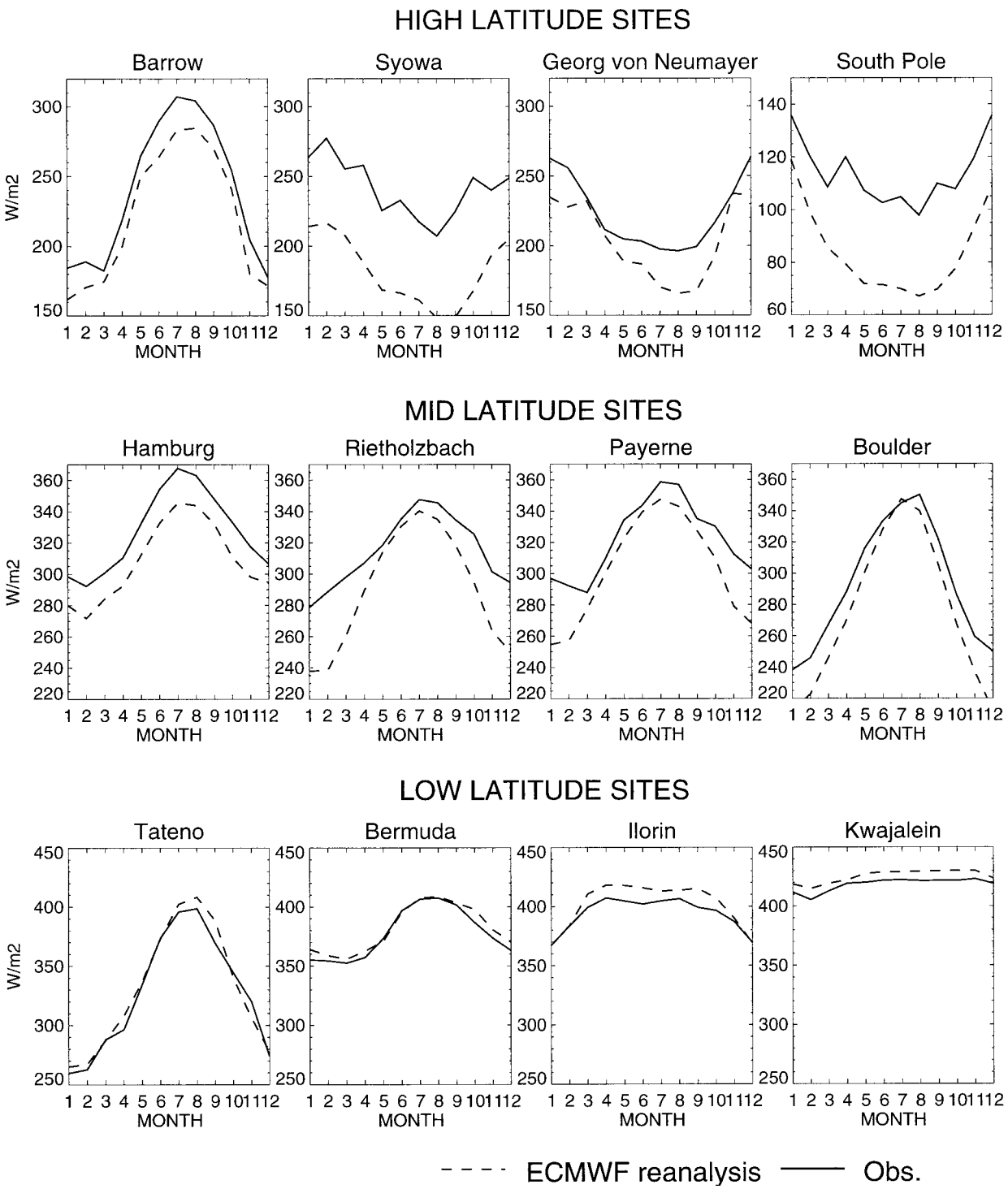

FIG. 8. As Fig. 4, but fluxes calculated by ERA.

better agreement or are slightly overestimated. Note that a similar tendency can also be detected on a seasonal basis at some of the sites, with larger biases in the cold season than in the warmer season (cf. e.g., the sites Boulder, Colorado; Payerne, Switzerland; South Pole in Fig. 8).

The similarity of the biases found in both ERA and GCMs confirms that the biases in DLR are not primarily

Unauthenticated | Downloaded 05/28/23 05:15 PM UTC

due to erroneous atmospheric input to the radiation scheme (which should be small in ERA), but rather are due to the radiation schemes themselves. This conclusion is further supported by independent stand-alone calculations for cloud-free conditions with the ERA radiation scheme, using the same atmospheric input from the four observation sites as before in Fig. 6. As with the two ECHAM radiation schemes, the ERA scheme underestimates particularly the emission of the cases with cold dry atmospheres from the sites in Greenland, Antarctica, and Payerne in winter, while the warm and humid cases from Payerne during summer and from Kwajalein are in better agreement or are slightly overestimated (Fig. 7b). These tendencies are then reflected in the biases in the long-term all-sky climatologies in Fig. 7a. Interestingly enough the slopes of the linear regression lines are almost identical in Figs. 7a and 7b, despite the independent underlying datasets of completely different spatial and temporal scales. The evident similarity of Figs. 7a and 7b is once again a strong indicator that the biases in the all-sky flux climatologies are to a large extent caused by biases in the clear-sky performance of the radiation scheme. Consistent results are given in Allan (2000) for the ERA fluxes at a tropical and a polar site, and in Chevallier and Morcrette (2000) for the fluxes of the ECMWF operational analysis as compared with surface observations from various sources.

The biases detected in the current study are strongly dependent on the water vapor content. A lack of thermal emission is calculated under dry conditions and slightly excessive emission under moist conditions. This suggests that it is primarily the dependence of DLR on the water vapor content that is not adequately captured in the radiation schemes. It is likely that these problems are related to the formulation of the water vapor continuum, which to date still poses the largest source of uncertainty in longwave radiation modeling.

In that respect there are some noteworthy changes from HadAM2b to HadAM3 that arise mainly from the clear-sky DLR. They are due to the inclusion of the Edwards and Slingo (1996) radiation scheme in HadAM3 that, most important, uses the Clough–Kneizys–Davies (CKD) formulation of the water vapor continuum (Clough et al. 1989; Iacono et al. 2000). As compared with the scheme used in HadAM2b, this significantly reduces the DLR for warm, moist profiles and slightly increases the DLR for cold, dry profiles (cf. Fig. 19 of Pope et al. 2000). These effects are evident in Fig. 3 (bringing the slope of the linear least squares fit closer to one in HadAM3 than in HadAM2b) and Fig. 5.

The water vapor continuum in the radiation code used for the new 40-yr reanalysis project at ECMWF (ERA-40) has also been revised along the CKD approach. We found in stand-alone calculations that this revision reduced the biases with respect to synchronous radiation measurements significantly when compared with the earlier radiation codes used at ECMWF (not shown).

In terms of global means, the analyses suggest that the ERA value of 339 W m^{-2} poses rather a lower limit for a tentative ''true'' global mean DLR, since the slight overestimation at low-latitude sites can hardly make up for the substantial underestimation at higher latitudes (Fig. 7). GCMs with significantly lower global mean values than ERA (cf. Fig. 2) are thus likely to underestimate the DLR considerably. From the bias structure in the above comparisons, a global mean estimate of DLR close to the ECHAM4 value of 344 W m^{-2} may be considered most realistic (the overestimation in the Tropics in that model seems to be large enough to counterbalance the underestimation in the extratropics). This is also in line with the recent study of Gupta et al. (1999), who estimated the global mean DLR at 348 W m^{-2}. At the same time this illustrates that the simulation of a realistic global mean value of DLR in GCMs is a necessary but not sufficient prerequisite to obtain an adequate spatial distribution of the longwave fluxes at the surface.

6. Conclusions

Downward longwave radiation (DLR) climatologies have been assessed in four GCMs with four independent radiation schemes and in the ERA using direct observations. Based on a total of 45 worldwide distributed observation sites from the GEBA and BSRN databases, a tendency was found in the GCMs to underestimate the DLR. The best estimate given in the present study for global mean DLR is 344 W m^{-2}, a value higher than typically found in GCMs. However, it has been shown that this underestimation is not uniform over the globe, but depends systematically on the prevailing climatic conditions. Significant underestimates are found at observation sites in cold and dry climates with low DLR emission. This underestimation gradually diminishes at sites with more moderate climates, while at sites with warm and humid atmospheres and high DLR emission, the biases are small or even reversed in some of the models. This implies that the meridional gradient of DLR in the GCMs is excessively strong. The very same biases as in the GCMs are also found in the DLR fluxes calculated by the ERA, despite the observational constraints in its atmospheric temperature and humidity structure. This suggests that the significant biases in the GCM-simulated DLR climatologies are not primarily caused by biases in the model-predicted atmospheric temperature and humidity structure that enter the radiative transfer calculations, but rather are due to problems in the formulation of the radiation schemes themselves. This is supported by an independent stand-alone validation of the ECHAM and ECMWF radiation schemes for cloud-free conditions, which reveals very similar biases. Using observed clear-sky profiles of atmospheric temperature and humidity rather than GCM-predicted

Unauthenticated | Downloaded 05/28/23 05:15 PM UTC

atmospheric input, the radiation codes calculate too-small DLR when driven with atmospheric data from sites in high-latitude and midlatitude winter with cold, dry climates. Under hot and humid clear-sky conditions, however, the isolated radiation schemes calculate DLR fluxes in better agreement with the synchronous radiation observations, or even overestimate them, very similar to the biases in the flux climatologies of the fully three-dimensional GCMs. This suggests that the bias in the DLR climatologies in the GCMs is predominantly induced by problems of their radiation schemes to simulate the emission of the cloud-free atmosphere accurately. These problems become particularly evident under cold and dry conditions in the form of a substantially underestimated DLR.

There is some evidence that the underestimate of DLR for cold, dry climates is less serious for the more recent radiation codes used in ECHAM/ECMWF and HadAM3. In the case of HadAM3, this is because the Edwards and Slingo (1996) radiation scheme includes the CKD formulation of the water vapor continuum, which leads to an increase in the DLR for such conditions. This result is consistent with Iacono et al. (2000), who found a substantial increase in the DLR at high latitudes when they included the Rapid Radiative Transfer Model radiation code, which uses the CKD continuum, in the National Center for Atmospheric Research Community Climate Model. It is clearly important that climate models should include up-to-date radiation schemes in order to minimize such errors. Further comparisons between models and observations, particularly at high latitudes, are needed in order to determine the source of the errors discussed here.

Acknowledgments. Thanks to ECMWF, Reading, United Kingdom, and Rachel Stratton, Hadley Centre, Bracknell, United Kingdom, for providing the ERA and HadAM data within the framework of the EU project HIRETYCS. The work at the Institute for Climate Research ETH was supported by the Swiss Bundesamt für Bildung und Wissenschaft (BBW) Grant 95.0640. Special thanks to Dr. B. Cechet, CSIRO Division for Atmospheric Research, for providing the data from the Uardry site and A. Beljaars, ECMWF, for the Cabauw data. The Swiss Scientific Computing Center (CSCS) generously provided the necessary computer resources for the high-resolution ECHAM3 and ECHAM4 simulations.

REFERENCES

Allan, R. P., 2000: Evaluation of simulated clear-sky longwave radiation using ground-based observations. *J. Climate,* **13,** 1951–1964.

Chevallier, F., and J. J. Morcrette, 2000: Comparison of model fluxes with surface and top-of-the-atmosphere observations. *Mon. Wea. Rev.,* **128,** 3839–3852.

Clough, S. A., F. X. Kneizys, and R. W. Davies, 1989: Line shape and the water vapour continuum. *Atmos. Res.,* **23,** 229–241.

DeLuisi, J., K. Dehne, R. Vogt, T. Konzelmann, and A. Ohmura, 1992: First results of the Baseline Surface Radiation Network (BSRN) broadband infrared radiometer intercomparison at FIR-EII. *Proc. Conf. Int. Rad. Symp.'92,* Tallin, Estonia, 559–564.

Edwards, J. M., and A. Slingo, 1996: Studies with a flexible new radiation code. I: Choosing a configuration for a large-scale model. *Quart. J. Roy. Meteor. Soc.,* **122,** 689–719.

Garratt, J. R., and A. J. Prata, 1996: Downwelling longwave fluxes at continental surfaces—A comparison with GCM simulations and implications for the global land-surface radiation budget. *J. Climate,* **9,** 646–655.

Gibson, R., P. Kallberg, S. Uppala, A. Hernandez, A. Nomura, and E. Serrano, 1997: ECMWF Re-Analysis project report series, Vol. 1. ERA description, ECMWF, Reading, 72 pp.

Gilgen, H., and A. Ohmura, 1999: The Global Energy Balance Archive. *Bull. Amer. Meteor. Soc.,* **80,** 831–850.

——, M. Wild, and A. Ohmura, 1998: Means and trends of shortwave irradiance at the surface estimated from Global Energy Balance Archive data. *J. Climate,* **11,** 2042–2061.

Giorgetta, M., and M. Wild, 1995: The water vapor continuum and its representation in ECHAM4. Max Planck Institute for Meteorology Rep. 162, 38 pp. [Available from MPI für Meteorologie, Bundesstr. 55, D-20146 Hamburg, Germany.]

Gupta, S. K., N. A. Ritchey, A. C. Wilber, and C. H. Whitlock, 1999: A climatology of surface radiation budget derived from satellite data. *J. Climate,* **12,** 2691–2710.

Gutowski, W. J., D. S. Gutzler, and W. C. Wang, 1991: Surface energy balances of three general circulation models: Implications for simulating regional climate change. *J. Climate,* **4,** 121–134.

Harrison, E. F., P. Minnis, B. R. Barkstrom, V. Ramanathan, R. D. Cess, and G. G. Gibson, 1990: Seasonal variation of cloud radiative forcing derived from the Earth Radiation Budget Experiment. *J. Geophys. Res.,* **95,** 18 687–18 703.

Hense, A., M. Kerschgens, and E. Raschke, 1982: An economical method for computing radiative transfer in circulation models. *Quart. J. Roy. Meteor. Soc.,* **108,** 231–252.

Iacono, M. J., E. J. Mlawer, S. A. Clough, and J. J. Morcrette, 2000: Impact of an improved longwave radiation model, RRTM, on the energy budget and thermodynamic properties of the NCAR community climate model, CCM3. *J. Geophys. Res.,* **105,** 14 873–14 890.

Ma, C. C., C. R. Mechoso, A. Arakawa, and J. D. Farrara, 1994: Sensitivity of a coupled atmosphere–ocean model to physical parameterizations. *J. Climate,* **7,** 1883–1896.

Morcrette, J. J., L. Smith, and Y. Fouquart, 1986: Pressure and temperature dependence of the absorption in longwave radiation parameterizations. *Beitr. Phys. Atmos.,* **59,** 455–469.

Ohmura, A., H. Gilgen, and M. Wild, 1989: Global Energy Balance Archive GEBA, World Climate Program Water Project A7, Geographical Writings of Zurich No. 34, Verlag der Fachvereine, 62 pp. [Available from Institute for Climate Research ETH, Winterthurerstr. 190; CH-8057 Zurich, Switzerland.]

——, T. Konzelmann, M. Rotach, J. Forrer, M. Wild, A. Abe-Ouchi, and H. Toritani, 1994: Energy balance for the Greenland ice sheet by observation and model computation. *Snow and Ice Covers: Interactions with the Atmosphere and Ecosystems,* H. G. Jones et al., Eds., IAHS (Publication No. 223), 85–95.

——, and Coauthors,1998: Baseline Surface Radiation Network (BSRN/WCRP): New precision radiometry for climate research. *Bull. Amer. Meteor. Soc.,* **79,** 2115–2136.

Philipona, R., and Coauthors,1998: The baseline surface radiation network pyrgeometer round-robin calibration experiment. *J. Atmos. Oceanic Technol.,* **15,** 687–696.

Pope, V. D., M. L. Gallani, P. R. Rowntree, and R. A. Stratton, 2000: The impact of new physical parameterizations in the Hadley Centre climate model: HadAM3. *Climate Dyn.,* **16,** 123–146.

Prata, A. J., I. F. Grant, R. P. Cechet, and G. F. Rutter, 1998: Five years of shortwave irradiances at a continental land site. *J. Geophys. Res.,* **103,** 26 093–26 106.

Randall, D. A., and Coauthors, 1992: Intercomparison and interpre-

Unauthenticated | Downloaded 05/28/23 05:15 PM UTC

tation of surface energy fluxes in atmospheric general circulation models. *J. Geophys. Res.,* **97,** 3711–3725.

Roeckner, E., and Coauthors,1992: Simulation of the present-day climate with the ECHAM model: Impact of model physics and resolution. Max Planck Institute for Meteorology Rep. 93, 171 pp. [Available from MPI für Meteorologie, Bundesstr. 55, D-20146 Hamburg, Germany.]

——, and Coauthors,1996: The atmospheric general circulation model ECHAM4: Model description and simulation of present day climate. Max Planck Institute for Meteorology Rep. 218, 130 pp. [Available from MPI für Meteorologie, Bundesstr. 55, D-20146 Hamburg, Germany.]

Shuttleworth, W. J., 1988: Evaporation from Amazonian rainforest. *Proc. Roy. Soc. London,* **B233,** 321–346.

Slingo, A., and R. C. Wilderspin, 1986: Development of a revised long-wave radiation scheme for an atmospheric general circulation model. *Quart. J. Roy. Meteor. Soc.,* **112,** 371–386.

Stratton, R. A., 1999: A high resolution AMIP integration using the Hadley Centre model HadAM2b. *Climate Dyn.,* **15,** 9–28.

Van Ulden, A. P., and J. Wieringa, 1996: Atmospheric boundary layer research at Cabauw. *Bound.-Layer Meteor.,* **78,** 39–69.

Wild, M., 1997: The heat balance of the Earth in GCM simulations of present and future climate. Verlag der Fachvereine, Zurich Climatological Rep. 68, 188pp. [Available from Institute for Climate Research ETH, Winterthurerstr. 190; CH-8057 Zurich, Switzerland.]

——, A. Ohmura, H. Gilgen, and E. Roeckner, 1995a: Validation of GCM simulated radiative fluxes using surface observations. *J. Climate,* **8,** 1309–1324.

——, ——, ——, and ——, 1995b: Regional climate simulation with a high resolution GCM: Surface radiative fluxes. *Climate Dyn.,* **11,** 469–486.

——, ——, and U. Cubasch, 1997: GCM simulated surface energy fluxes in climate change experiments. *J. Climate,* **10,** 3093–3110.

——, ——, H. Gilgen, E. Roeckner, M. Giorgetta, and J. J. Morcrette, 1998: The dispostion of radiative energy in the global climate system: GCM-calculated versus observational estimates. *Climate Dyn.,* **14,** 853–869.

Unauthenticated | Downloaded 05/28/23 05:15 PM UTC